Korean J. Chem. Eng., 35(12), 2496-2503 (2018)
DOI: 10.1007/s11814-018-0154-1

pISSN: 0256-1115
eISSN: 1975-7220

Investigation of short-term stability in high efficiency polymer : nonfullerene solar cells via quick current-voltage cycling method

Sooyong Lee*, Jooyeok Seo*, Hwajeong Kim*,,†, Dong-Ik Song***, and Youngkyoo Kim*,†**

*Organic Nanoelectronics Laboratory and KNU Institute for Nanophotonics Applications (KINPA), Department of Chemical Engineering, School of Applied Chemical Engineering, Kyungpook National University, Daegu 41566, Korea
**Research Institute of Advanced Energy Technology, Kyungpook National University, Daegu 41566, Korea
***Polymer Rheology Laboratory, Department of Chemical Engineering, School of Applied Chemical Engineering, Kyungpook National University, University Road 80, Daegu 41566, Korea
(*Received 27 April 2018 • accepted 18 September 2018*)

Abstract—The short-term stability of high efficiency polymer : nonfullerene solar cells was investigated by employing a quick (ten cycles) current density-voltage (J-V) cycling method. Polymer : nonfullerene solar cells with initial power conversion efficiency (PCE) of >10% were fabricated using bulk heterojunction (BHJ) films of poly[(2,6-(4,8-bis(5-(2-ethylhexyl)thiophen-2-yl)-benzo[1,2-b:4,5b′]dithiophene))-alt-(5,5-(1′,3′-di-2-thienyl-5,7′-bis(2-ethylhexyl)benzo[1′,2′-c:4′,5′-c′]dithiophene-4,8-dione))] (PBDB-T) and 3,9-bis(2-methylene-((3-(1,1-dicyanomethylene)-6/7-methyl)-indanone))-5,5,11,11-tetrakis(4-hexylphenyl)-dithieno[2,3-d:2′,3′-d′]-s-indaceno[1,2-b:5,6-b′]dithiophene (IT-M). One set of the BHJ (PBDB-T : IT-M) films was thermally annealed at 160 °C for 30 min, while another set was used without any thermal treatment after spin-coating. The quick J-V scan (cycling) measurement disclosed that the PCE decay was relatively slower for the annealed BHJ layers than the unannealed (as-cast) BHJ layers. As a result, after ten cycles, the annealed BHJ layers delivered higher PCE than the unannealed BHJ layers due to higher and more stable trend in fill factor. The present quick J-V cycling method is simple but expected to be useful for the prediction of short-term stability in organic solar cells.

Keywords: Organic Solar Cells, Bulk Heterojunction, Nonfullerene, PBDB-T : IT-M, Stability

INTRODUCTION

Organic solar cells have been extensively highlighted for the past two decades because of their potential for realizing clean energy (electricity) by utilizing a variety of organic semiconducting materials [1-3], even though other desirable methods including biodiesels have been also proposed [4-7]. In particular, organic solar cells have further advantages including quick energy payback time [8-11] and viability for flexible/rollable plastic solar modules like wall papers [12-14]. To date, most high efficiency organic solar cells have been fabricated by employing bulk heterojunction (BHJ) layers that consist of electron-donating and electron-accepting organic materials [15-19]. The BHJ layers benefit in that the charge separation yield from excitons generated upon solar light illumination could be maximized at the donor-acceptor interfaces on the nanoscale [20-26]. Of various material combinations for the BHJ layers, polymer : fullerene BHJ layers have been intensively studied owing to the excellent electron-accepting role of fullerene derivatives leading to high power conversion efficiency (PCE) [27-38].

However, the low stability of polymer : fullerene solar cells has been an issue due partly to the morphological instability caused by the migration or movement of fullerene derivatives during operation [39-45], because fullerene derivatives have a tendency to make crystallites by themselves [46-49]. On this account, nonfullerene acceptors have attracted keen interest and their better light-harvesting characteristics in the longer wavelengths, compared to fullerene derivatives, contributed to achieving high PCEs exceeding 10% [50-54]. These nonfullerene acceptors, however, are also in a category of small molecules, even though they have a planar backbone structure unlike the ball shape of fullerene derivatives. Therefore, it is necessary to investigate the stability of polymer : nonfullerene solar cells, but only a couple of storage [55-59] and thermal (oxidative) stability without continuous illumination of solar light have been reported so far [60-63].

Here it is understood that the long-term stability investigation of solar cells needs considerable efforts including long time measurements by applying durable solar simulators etc. In this regard, a short-term lifetime test has been employed for the investigation of early stage stability [64-70]. However, less attention has been paid to the electrical sweep test in organic solar cells, including polymer : nonfullerene solar cells, even though the current density-voltage (J-V) characteristics of organic solar cells upon repeated sweeps can provide a fingerprint diagnosing the state of devices, which eventually affects the stability of solar cells. Therefore, the quick J-V measurement can be a simple but an effective method to examine the initial stability of organic solar cells.

†To whom correspondence should be addressed.
E-mail: ykimm@knu.ac.kr, khj217@knu.ac.kr

In this work, we attempted to investigate the short-term stability of inverted-type polymer : nonfullerene solar cells from the J-V curves measured upon quick sweep (initial ten cycles) under illumination with a simulated solar light (100 mW/cm^2, air mass 1.5 G). The polymer : nonfullerene solar cells were fabricated with the BHJ layers of poly[(2,6-(4,8-bis(5-(2-ethylhexyl)thiophen-2-yl)-benzo[1,2-b:4,5-b′]dithiophene))-alt-(5,5-(1′,3′-di-2-thienyl-5′,7′-bis(2-ethylhexyl)benzo[1′,2′-c:4′,5′-c′]dithiophene-4,8-dione))] (PBDB-T) and 3,9-bis(2-methylene-((3-(1,1-dicyanomethylene)-6/7-methyl)-indanone))-5,5,11,11-tetrakis(4-hexylphenyl)-dithieno[2,3-d:2′,3′-d′]-s-indaceno[1,2-b:5,6-b′]dithiophene (IT-M) as an electron donor and an electron acceptor, respectively. In particular, two types of the PBDB-T : IT-M solar cells, of which BHJ layers were either unannealed (as-cast) or annealed (at 160 °C for 30 min), were fabricated in order to understand the influence of thermal annealing on the short-term stability. Results showed that the annealed BHJ layers delivered better short-term stability than the unannealed BHJ layers even though the initial PCE was marginally lower for the annealed BHJ layers.

EXPERIMENTAL

PBDB-T (weight-average molecular weight=18 kDa; polydispersity index=2.5) and IT-M (formula weight=1.455 kDa) were used as received from Solarmer (USA), respectively. Zinc acetate dehydrate (purity >99%) was purchased from Sigma-Aldrich (USA) and used for the preparation of zinc oxide (ZnO) electron-collecting buffer layers for inverted-type organic solar cells. Blend solutions of PBDB-T and IT-M were prepared using chlorobenzene (CB) as a solvent and 1,8-diiodooctane (DIO, 1.0 vol%) as an additive at a solid concentration of 20 mg/ml (PBDB-T : IT-M=1 : 1 by weight). These solutions were subjected to stirring for better mixing at room temperature for three days prior to spin-coating. The ZnO precursor solutions were prepared by dissolving zinc acetate dehydrate (100 mg) in the mixture of 2-methoxyethanol (1 ml) and ethanol amine (0.028 ml, stabilizer), followed by stirring at 60 °C for 3 h and then at room temperature for 12 h.

Prior to the fabrication of PBDB-T : IT-M solar cells, indium-tin oxide (ITO)-coated glass substrates were patterned to make the ITO stripes on the glass substrates. After cleaning the patterned ITO-glass substrates using acetone and isopropyl alcohol in an ultrasonic cleaner, a nitrogen gas flow was applied to dry the wet-cleaned ITO-glass substrates. Finally, a UV-ozone cleaner was used to treat the surface of the dried ITO-glass substrates for 20 min. Next, the ZnO precursor solutions were spun on the ITO-glass substrates (the ITO side), followed by annealing at 200 °C for 1 h in air ambient

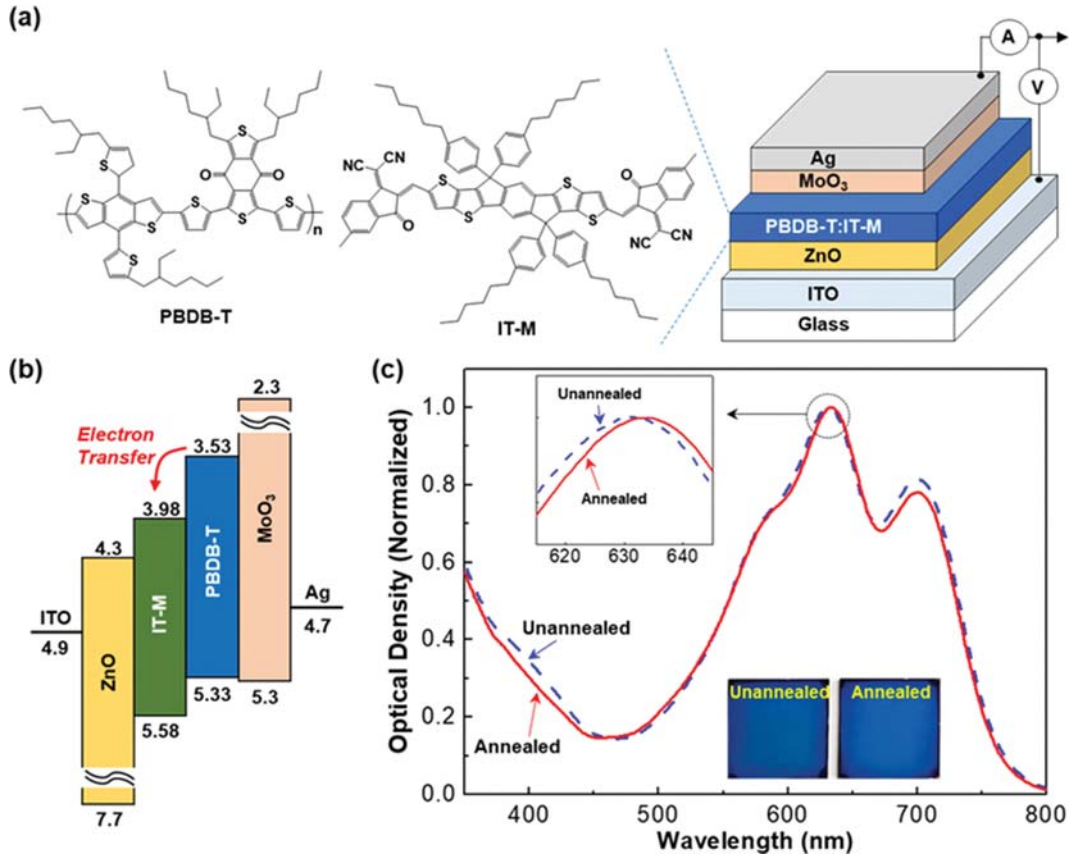

Fig. 1. (a) Device structure for the inverted-type organic solar cells with the PBDB-T : IT-M BHJ layers and chemical structures of materials used in this work. (b) Simplified flat energy band diagram for the PBDB-T : IT-M solar cells (note that the 'eV' unit and minus sign in the energy values are omitted). (c) Optical absorption spectra for the PBDB-T : IT-M BHJ films (see the inset photograph) before and after thermal annealing at 160 °C for 30 min.

condition. After cooling the ZnO/ITO-glass substrates, the PBDB-T : IT-M BHJ layers were spin-coated on the ZnO layers in the glove box charged with nitrogen gas. One set of the samples was thermally annealed on a hot plate at 160 °C for 30 min inside a nitrogen-charged glove box. All the film-coated samples were transferred to a vacuum chamber system equipped inside an argon-charged glove box. After the base pressure of chamber reached ~1.0×10^{-6} torr, molybdenum oxide (MoO_3, 10 nm) and silver (Ag, 80 nm) electrodes were subsequently deposited on the PBDB-T : IT-M layers by thermal evaporation. The fabricated devices, glass/ITO/ZnO/PBDB-T : IT-M/MoO_3/Ag, were stored in the same argon-filled glove box to protect from the possible attack by moisture and oxygen.

The film thickness was measured using a surface profiler (Alpha Step 200, Tencor), while the optical absorption spectra of films were measured using a UV-visible spectrophotometer (Lambda 750, PerkinElmer). The solar cell performance of devices was measured using a home-built solar cell measurement system equipped with a solar simulator (92250A-1000, Newport Oriel) and an electrometer (Keithley 2400). The incident light intensity was 100 mW/cm^2 (air mass 1.5 G), which was controlled by using a calibrated reference cell certified by BS-520 (Bunkoukeiki). For the sweep test, the voltage applied to the PBDB-T : IT-M solar cells was increased from −1 V to 1 V at a ramp rate of 0.01 V/s. All devices were measured under an inert environment at room temperature as they were mounted and tightly shielded inside a sample holder filled with argon gas.

RESULTS AND DISCUSSION

As shown in Fig. 1(a), both PBDB-T and IT-M have a few alkyl chains which play an important role in bestowing solubility in organic (nonpolar) solvents. However, if both PBDB-T and IT-M molecules are not tightly stacked in a solid-state film, the alkyl chains are considered to act as an electrical insulator and disturb the effective charge transfer between the two molecules. In addition, if such an imperfect molecular stacking between PBDB-T and IT-M is randomly present in the BHJ (PBDB-T : IT-M) layers of the inverted-type organic solar cells (see the device structure in Fig. 1(a)), the molecular morphology in the BHJ layers is likely to easily change during the excitation-charge separation-charge transport processes. As a consequence, the electron transfer and/or charge transport in the BHJ layers can be unstable with time (see the flat energy band diagram in Fig. 1(b)). Given that both PBDB-T and IT-M molecules are mixed in the BHJ layers for the present device structure, a feasible way is to thermally anneal the BHJ layers for improving their molecular stacking as well documented in other types of solar cells [71-74]. As shown in Fig. 1(c), it is considered that the optical absorption spectrum of the PBDB-T : IT-M (1 : 1 by weight) films was very marginally changed by thermal annealing at 160 °C for 30 min. However, a close look into the peak region between 600 nm and 650 nm (wavelength) reveals that the maximum absorption peak was obviously red-shifted by thermal annealing. Note that the thermal annealing slightly changed the film color from bluish-green jade to bluish (see the inset photograph in Fig. 1(c)). This result indicates that the better molecular stacking in the BHJ layers might be made by the thermal annealing process because

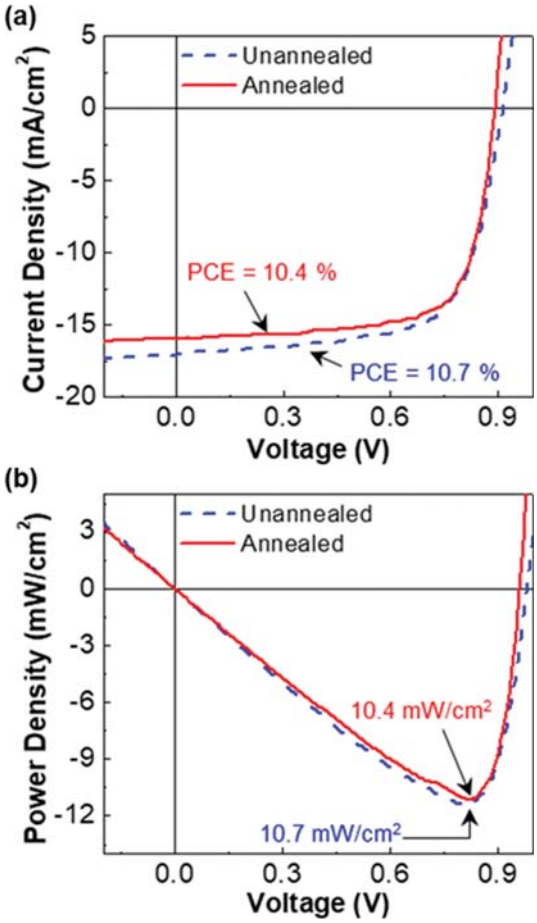

Fig. 2. (a) Current density-voltage (J-V) curves and (b) power density-voltage curves under illumination with a simulated solar light (air mass 1.5 G, 100 mW/cm^2) for the PBDB-T : IT-M solar cells before (unannealed) and after (annealed) thermal annealing of the BHJ layers.

the red-shift phenomenon does typically occur in the case of an extended conjugation length etc.

As shown in Fig. 2(a), the devices with the unannealed BHJ (PBDB-T : IT-M) layers delivered slightly better J-V characteristics than those with the annealed BHJ layers. This result implies that

Table 1. Solar cell parameters for the PBDB-T : IT-M solar cells with the unannealed (as-cast) and annealed BHJ layers. J_{SC}, V_{OC}, FF, PCE, R_S, and R_{SH} denote short circuit current density, open circuit voltage, power conversion efficiency, series resistance, and shunt resistance, respectively

Parameters	PBDB-T : IT-M (BHJ)	
	Unannealed (as-cast)	Annealed (160 °C/30 min)
J_{SC} (mA/cm^2)	17.1 (±0.3)	15.9 (±0.2)
V_{OC} (V)	0.93 (±0.01)	0.91 (±0.01)
FF (%)	67.7 (±1.1)	71.8 (±0.9)
PCE (%)	10.7 (±0.2)	10.4 (±0.3)
R_S (kΩ·cm^2)	0.07 (±0.01)	0.04 (±0.01)
R_{SH} (kΩ·cm^2)	4.7 (±0.6)	2.4 (±0.7)

the performance of solar cells was slightly lowered by the thermal annealing process. As summarized in Table 1, both short circuit current density (J_{SC}) and open circuit voltage (V_{OC}) was reduced after thermal annealing. As a result, the PCE was decreased from 10.7% to 10.4% by the thermal annealing process. The reason for the slightly lowered PCE can be attributable to the changed morphology leading to the better molecular stacking as supported by the optical absorption spectra discussed above. In addition, it is also considered that the extraction (movement) of additive (DIO) molecules might result in the reduced performance because DIO is a liquid with soft alkane group. However, interestingly, the fill factor (FF) was rather noticeably increased from 67.7% to 71.8%. This result indicates the improved charge transfer inside the BHJ layers, even though overall number of charges generated was slightly reduced leading to the marginally reduced maximum power density ($P_{MAX}=J_{SC}\cdot V_{OC}\cdot FF$) (see Fig. 2(b)).

Next, the PBDB-T : IT-M solar cells were subjected to the continuous sweep measurement of J-V curves by repeating ten cycles from −1.0 V to +1.0 V at a ramp rate of 0.01 V/s. As the cycle number (No.) increased, the J-V curves became slightly poorer in the presence of the J_{SC} reduction irrespective of thermal annealing (see Fig. 3(a), (b)). This is clearly observed from the enlarged graph in the inset of Fig. 3. However, relatively small change in the J-V curves after ten cycles was measured for the devices with the annealed BHJ layers than the unannealed BHJ layers. This result means that the annealed BHJ layers are relatively more stable than the unannealed BHJ layers.

For a detailed investigation of the performance change in the devices with the unannealed and annealed BHJ layers, the J-V and power density curves were compared at the same cycle number. As

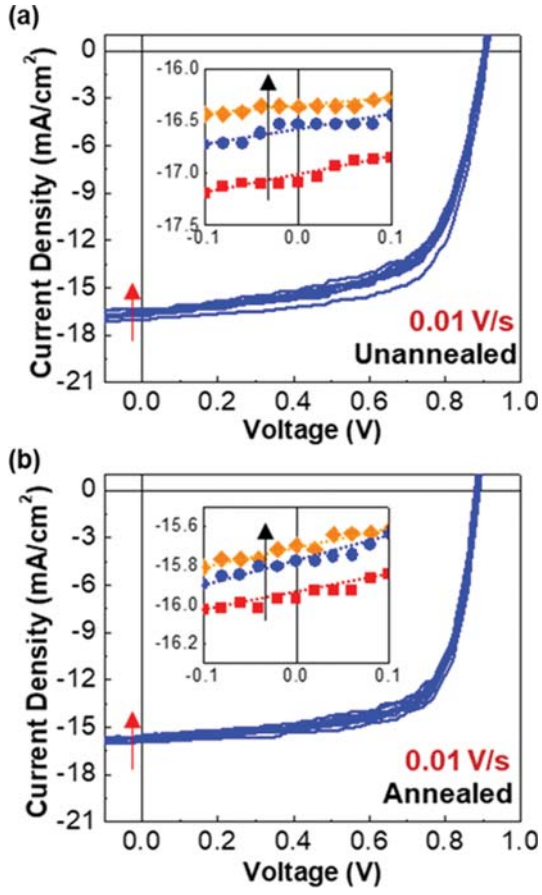

Fig. 3. Current density-voltage (J-V) curves by repeating 10 cycles from −1.0 V to +1.0 V at a ramp rate of 0.01 V/s under illumination with a simulated solar light (air mass 1.5 G, 100 mW/cm^2) for the PBDB-T : IT-M solar cells: (a) Unannealed BHJ layers, (b) annealed BHJ layers. Inset graphs show the enlarged data at around short circuit condition: Cycle number=1 (squares), 5 (circles), 10 (diamonds).

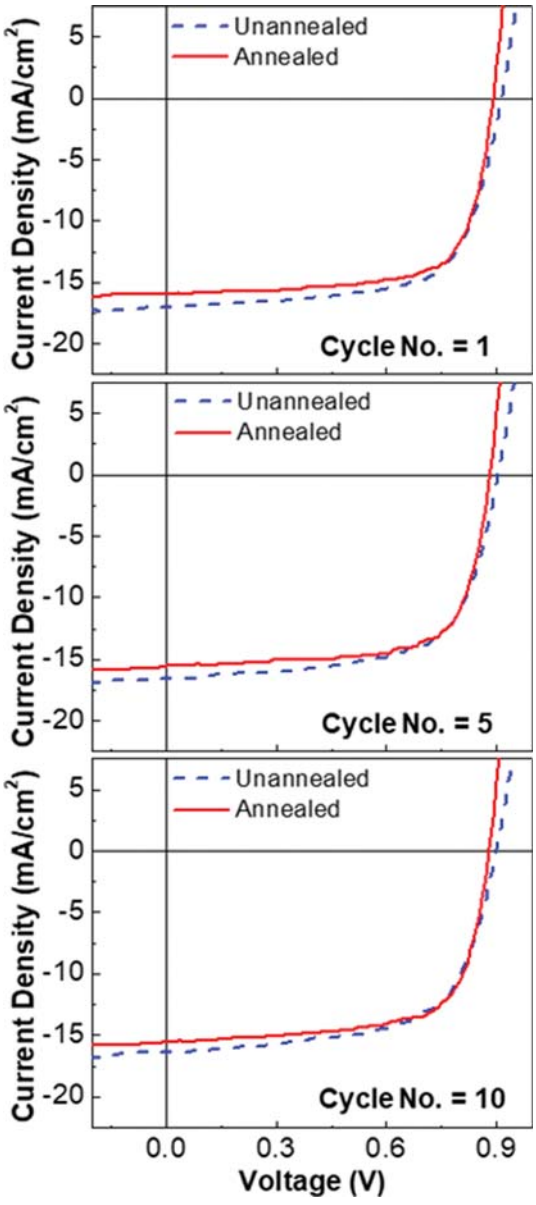

Fig. 4. Comparison of current density-voltage (J-V) curves at the same cycle number (No.) under illumination with a simulated solar light (air mass 1.5 G, 100 mW/cm^2) for the PBDB-T : IT-M solar cells with the unannealed (dashed line) and annealed (solid line) BHJ layers. Note that the power density values are given in blue and red color for the unannealed and annealed BHJ layers, respectively.

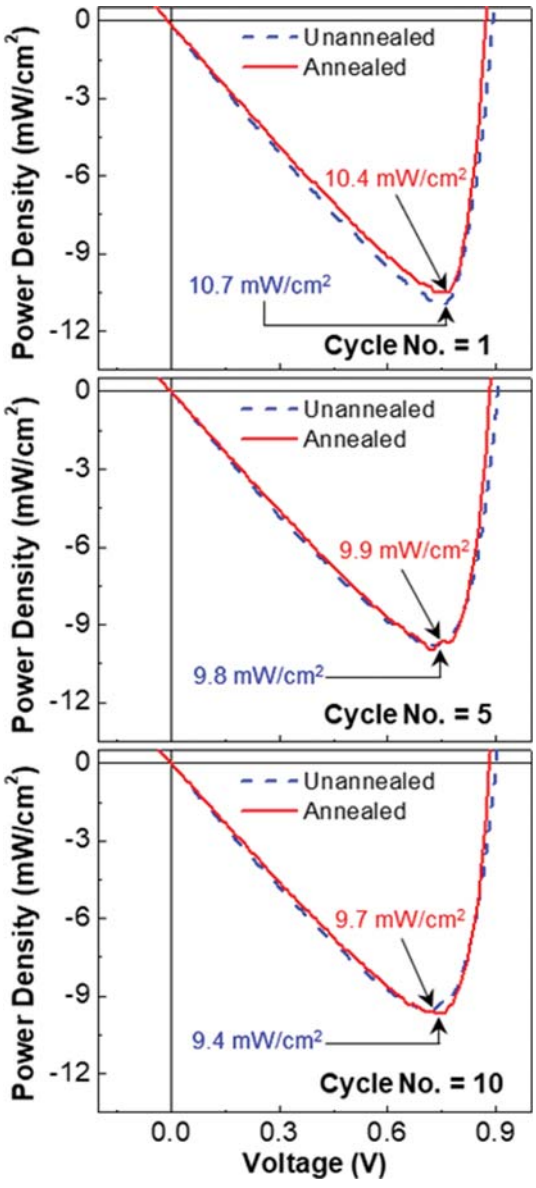

Fig. 5. Comparison of power density curves at the same cycle number under illumination with a simulated solar light (air mass 1.5 G, 100 mW/cm^2) for the PBDB-T : IT-M solar cells with the unannealed (dashed line) and annealed (solid line) BHJ layers.

shown in Fig. 4, the overall J-V curves were slightly better for the unannealed BHJ layers than the annealed BHJ layers at each cycle number. However, the gap of current density became gradually narrower as the cycle number increased because the deterioration in the J-V curves was relatively larger in the case of the unannealed BHJ layers than the annealed BHJ layers. Consequently, as shown in Fig. 5, the resulting maximum power density (P_{MAX}) after ten cycles was higher for the devices with the annealed BHJ layers (9.7 mW/cm^2) than those with the unannealed BHJ layers (9.4 mW/cm^2).

Finally, major solar cell parameters were plotted as a function of cycle number according to the thermal annealing. As shown in Fig. 6, both J_{SC} and V_{OC} gradually decreased as the cycle number increased. Interestingly, even after ten cycles, the J_{SC} and V_{OC} values were higher for the unannealed BHJ layers than the annealed BHJ layers. This result can support the fact that the optimum charge generation/separation morphology was made by the presence of DIO upon spin-coating, but the thermal annealing at 160 °C might alter the preset morphology by affecting the soft (thermally unstable) DIO molecules.

A similar decreasing trend was measured for FF, but the decreasing rate was relatively slower for the annealed BHJ layers than the unannealed BHJ layers. In contrast to the J_{SC} and V_{OC} values, the FF values were still higher for the annealed BHJ layers than the unannealed BHJ layers. The small change in FF for the annealed BHJ layers can be explained by the better molecular stacking upon thermal annealing, which might enable molecules (PBDB-T and IT-M) to bind more tightly, leading to a stable solid-state layer. As a result, the PCE value after ten cycles could be slightly higher for the annealed BHJ layers than the unannealed BHJ layers. A similar trend was measured for the maximum power density (P_{MAX}). Therefore, it is concluded that the stability of the present PBDB-T : IT-M solar cells could be improved by applying thermal annealing process for the BHJ layers. To further understand the rationale behind the stability cross-over, the electrical resistances of solar cells were extracted from the light J-V curves.

As shown in Fig. 7, a marginal increase in series resistance (R_S) was measured similarly for both the unannealed and annealed BHJ layers. However, the shunt resistance (R_{SH}) was more pronouncedly decreased for the unannealed BHJ layers than the annealed BHJ layers. This result informs that the physical leakage pathways might be relatively easily generated because of the rela-

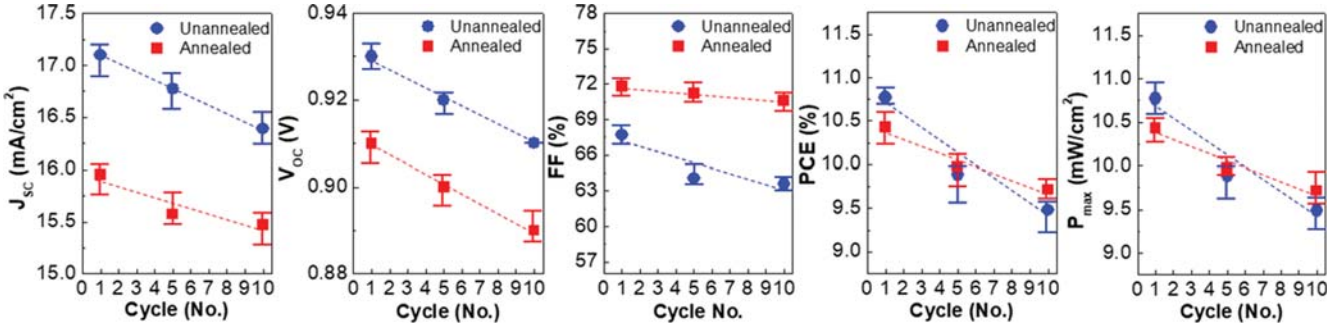

Fig. 6. Solar cell parameters (air mass 1.5 G, 100 mW/cm^2) as a function of the cycle number for the PPBDB-T : IT-M solar cells with the unannealed (filled circles) and annealed (filled squares) BHJ layers.

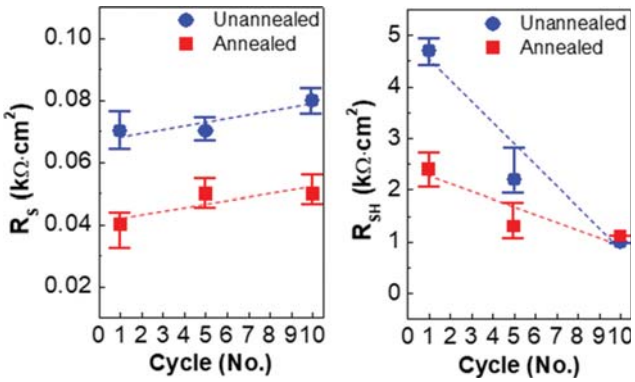

Fig. 7. Series resistance (R_S, left) and shunt resistance (R_{SH}, right) as a function of the cycle number for the PPBDB-T : IT-M solar cells with the unannealed (filled circles) and annealed (filled squares) BHJ layers.

Table 2. Solar cell parameters before (1st cycle) and after quick scan (10th cycle) for the PBDB-T : IT-M solar cells with the unannealed (as-cast) and annealed BHJ layers

Parameters	Unannealed (as-cast)		Annealed (160 °C/30 min)	
	1st cycle	10th cycle	1st cycle	10th cycle
J_{SC} (mA/cm^2)	17.1	16.4	16.0	15.4
V_{OC} (V)	0.93	0.91	0.91	0.89
FF (%)	67.7	63.6	71.8	70.6
PCE (%)	10.7	9.5	10.4	9.7
R_S (kΩ·cm^2)	0.07	0.08	0.04	0.05
R_{SH} (kΩ·cm^2)	4.7	1.0	2.4	1.1

tively poor molecular stacking in the unannealed BHJ layers, leading to the larger reduction in FF. So, the annealed BHJ layers have better molecular stacking, leading to relatively low probability of making physical leakage pathways, so that their solar cells could be more stable. Therefore, this result supports that the key information (device parameters) on the initial stability of organic solar cells can be delivered by the present J-V cycling measurement (see Table 2).

CONCLUSION

The short-term stability of the inverted-type PBDB-T : IT-M solar cells was investigated by employing the quick J-V scan (initial 10 cycles) method under continuous illumination with the simulated solar light (100 mW/cm^2, air mass 1.5 G). For comparison, both unannealed and annealed BHJ (PBDB-T : IT-M) layers were used for the fabrication of solar cells. The optical absorption spectra revealed that the maximum absorption peak of the BHJ layers was slightly red-shifted by the thermal annealing process, which led to marginally reduced PCE from 10.7% to 10.4%. The FF value was rather improved by thermal annealing, even though both J_{SC} and V_{OC} showed lower values in the case of the annealed BHJ layers. The higher the cycle number, the poorer the J-V curves. The degradation rate was relatively larger for the unannealed BHJ layers than the annealed BHJ layers. As a result, after ten cycles, the PCE value became higher for the annealed BHJ layers, even though it was lower initially. FF was assigned as a major parameter, which contributed to the relatively higher PCE for the annealed BHJ layers, because it was always higher and exhibited pronouncedly slow decreasing trend for the annealed BHJ layers. The detailed analysis disclosed that the huge reduction in R_{SH} by the physical leakage pathways was responsible for the relatively large FF decrease in the unannealed BHJ layers. Hence, the present J-V cycling method under continuous illumination of solar light is expected to be useful for the prediction of short-term stability (initial screening test) in organic solar cells.

ACKNOWLEDGEMENT

This work was financially supported by the National Research Foundation (NRF) of Korea (2016H1D5A1910319, 2018R1D1A1B07051075, 2017M2A2A4A01071010, 2018R1D1A3B07046214, Basic Science Research Program_ 2018R1A6A1A03024962).

REFERENCES

1. S. Chu, Y. Cui and N. Liu, *Nat. Mater.*, **16**, 16 (2017).
2. M. M. Aman, K. H. Solangi, M. S. Hossain, A. Badarudin, G. B. Jasmon, H. Mokhlis, A. H. A. Baker and S. N. Kazi, *Renew. Sust. Energy Rev.*, **41**, 1190 (2015).
3. I. Dincer and C. Acar, *Int. J. Energy Res.*, **39**, 585 (2015).
4. J. E, M. Pham, Y. Deng, T. Nguyen, V. Duy, D. Le, W. Zuo, Q. Peng and Z. Zhang, *Energy*, **149**, 979 (2018).
5. Z. Zhang, J. E, Y. Deng, M. H. Pham, W. Zuo, Q. Peng and Z. Yin, *Energy Convers. Manage.*, **159**, 244 (2018).
6. Y. Li, L. Meng, K. Nithyanandan, T. H. Lee, Y. Lin, C. F. Lee and S. Lia, *Fuel*, **184**, 864 (2016).
7. T. Liu, J. E, W. M. Yang, Y. Deng, H. An, Z. Zhang and M. Pham, *Energy*, **150**, 1031 (2018).
8. T. Ameri, N. Lia and C. J. Brabec, *Energy Environ. Sci.*, **6**, 2390 (2013).
9. L. Lu and L. Yu, *Adv. Mater.*, **26**, 4413 (2014).
10. H. Kim, S. Nam, J. Jeong, S. Lee, J. Seo, H. Han and Y. Kim, *Korean J. Chem. Eng.*, **31**, 1095 (2014).
11. A. Facchetti, *Mater. Today*, **16**, 123 (2013).
12. S. B. Darling and F. You, *RSC Adv.*, **3**, 17633 (2013).
13. A. J. Heeger, *Adv. Mater.*, **26**, 10 (2014).
14. J. Yan and B. R. Saunders, *RSC Adv.*, **4**, 43286 (2014).
15. S. Woo, W. Kim, H. Kim, Y. Yi, H. Lyu and Y. Kim, *Adv. Energy Mater.*, **4**, 1301692 (2014).
16. N. Wang, Z. Chen, W. Wei and Z. Jiang, *J. Am. Chem. Soc.*, **135**, 17060 (2013).
17. F. Padinger, R. S. Rittberger and N. S. Sariciftci, *Adv. Funct. Mater.*, **13**, 85 (2003).
18. T. L. Nguyen, H. Choi, S. Ko, M. A. Uddin, B. Walker, S. Yum, J. Jeong, M. H. Yun, T. J. Shin, S. Hwang, J. Y. Kim and H. Y. Woo, *Energy Environ. Sci.*, **7**, 3040 (2014).
19. M. Zhang, Y. Gu, X. Guo, F. Liu, S. Zhang, L. Huo, T. P. Russell and J. Hou, *Adv. Mater.*, **25**, 4944 (2013).
20. Y. Kim, S. A. Choulis, J. Nelson, D. D. C. Bradley, S. Cook and J. R. Durrant, *Appl. Phys. Lett.*, **86**, 063502 (2005).

21. Y. Deng, J. Liu, J. Wang, L. Liu, W. Li, H. Tian, X. Zhang, Z. Xie, Y. Geng and F. Wang, *Adv. Mater.*, **26**, 471 (2014).
22. M. Reyes-Reyes, K. Kim and D. L. Carroll, *Appl. Phys. Lett.*, **87**, 083506 (2005).
23. S. E. Shaheen, C. J. Brabec, N. S. Sariciftci, F. Padinger, T. Fromherz and J. C. Hummelen, *Appl. Phys. Lett.*, **78**, 841 (2001).
24. X. Guo, N. Zhou, S. J. Lou, J. Smith, D. B. Tice, J. W. Hennek, R. P. Ortiz, J. T. L. Navarrete, S. Li, J. Strzalka, L. X. Chen, R. P. H. Chang, A. Facchetti and T. J. Marks, *Nat. Photonics*, **7**, 825 (2013).
25. Y. Kim, S. Cook, S. M. Tuladhar, S. A. Choulis, J. Nelson, J. R. Durrant, D. D. C. Bradley, M. Giles, I. McCulloch, C. S. Ha and M. Ree, *Nat. Mater.*, **5**, 197 (2006).
26. S. Nam, J. Seo, H. Han, H. Kim, S. G. Hahm, M. Ree, Y. Gal, T. D. Anthopoulos, D. D. C. Bradley and T. Kim, *Adv. Mater. Interfaces*, **3**, 1600415 (2016).
27. S. Nam, J. Seo, S. Woo, W. H. Kim, H. Kim, D. D. C. Bradley and Y. Kim, *Nat. Commun.*, **6**, 8929 (2015).
28. C. J. Brabec, S. Gowrisanker, J. J. M. Halls, D. Laird, S. Jia and S. P. Willams, *Adv. Mater.*, **22**, 3839 (2010).
29. E. T. Hike, K. Vandewal, J. A. Bartelt, W. R. Mateker, J. D. Douglas, R. Moriefa, K. R. Graham, J. M. Fréchet, A. Salleo and M. D. McGehee, *Adv. Energy Mater.*, **3**, 220 (2013).
30. S.-H. Liao, H.-J. Jhuo, Y.-S. Cheng and S.-A. Chen, *Adv. Mater.*, **25**, 4766 (2013).
31. J. M. Lobez, T. L. Andrew, V. Bulović and T. M. Swager, *ACS Nano*, **6**, 3044 (2012).
32. T. Salim, H.-W. Lee, L. H. Wong, J. H. Oh, Z. Bao and Y. M. Lam, *Adv. Funct. Mater.*, **26**, 51 (2016).
33. M. C. Scharber, *Adv. Mater.*, **28**, 1994 (2016).
34. J. Seo, S. Park, M. Song, J. Jeong, C. Lee, H. Kim and Y. Kim, *Molecules*, **22**, 262 (2017).
35. N. Y. Doumon, G. Wang, R. C. Chiechi and L. J. A. Koster, *J. Mater. Chem. C*, **5**, 6611 (2017).
36. S. Albrecht, K. Vandewal, J. R. Tumbleston, F. S. U. Fischer, J. D. Douglas, J. M. J. Fréchet, S. Ludwigs, H. Ade, A. Salleo and D. Neher, *Adv. Mater.*, **26**, 2533 (2014).
37. R. Xia, D.-S. Leem, T. Kirchartz, S. Spencer, C. Murphy, Z. He, H. Wu, S. Su, Y. Cao, J. S. Kim, J. C. deMello, D. D. C. Bradley and J. Nelson, *Adv. Energy Mater.*, **3**, 718 (2013).
38. M. Song, S. Lee, D. Kim, C. Lee, J. Jeong, J. Seo, H. Kim, D.-I. Song, D. Kim and Y. Kim, *Energies*, **10**, 1886 (2017).
39. E. Collado-Fregoso, S. N. Hood, B. C. Schroeder, I. McCulloch, I. Kassal, D. Neher and J. R. Durrant, *J. Phys. Chem. Lett.*, **8**, 4061 (2017).
40. P. Cheng and X. Zhan, *Chem. Soc. Rev.*, **45**, 2544 (2016).
41. V. Coropeanu and J. Bredas, *J. Phys. Chem. C*, **121**, 24954 (2017).
42. P. Cheng, C. Yan, Y. Wu, J. Wang, M. Qin, Q. An, J. Cao, L. Huo, F. Zhang, L. Ding, Y. Sun, W. Ma and X. Zhan, *Adv. Mater.*, **28**, 8021 (2016).
43. A. Serbenta, O. V. Kozlov, G. Portale, P. H. M. Loosdrecht and M. S. Pshenichnikov, *Sci. Rep.*, **6**, 36236 (2016).
44. P. Cheng, C. Yan, T.-K. Lau, J. Mai, X. Lu and X. Zhan, *Adv. Mater.*, **28**, 5822 (2016).
45. W. Huang, E. Gann, Y.-B. Cheng and C. R. McNeill, *ACS Appl. Mater. Interfaces*, **7**, 14026 (2015).
46. M. Qin, P. Cheng, J. Mai, T.-K. Lau, Q. Zhang, J. Wang, C. Yan, K. Liu, C.-J. Su, W. You, X. Lu and X. Zhang, *Sol. RRL*, **1**, 1700148 (2017).
47. W. Huang, N. Chandrasekaranm, S. K. K. Prasad, E. Gann, L. Thomsen, D. Kabra, J. M. Hodgkiss, Y.-B. Cheng and C. R. McNeill, *ACS Appl. Mater. Interfaces*, **8**, 29608 (2016).
48. X. Zhang, D. Zheng, S. Xing, H. Wang, J. Huang and J. Yu, *Sol. Energy*, **147**, 106 (2017).
49. F. Liu, D. Chen, C. Wang, K. Luo, W. Gu, A. L. Briseno, J. W. P. Hsu and T. P. Russell, *ACS Appl. Mater. Interfaces*, **6**, 19876 (2014).
50. S. Li, L. Ye, W. Zhao, S. Zhang, S. Mukherjee, H. Ade and J. Hou, *Adv. Mater.*, **28**, 9423 (2016).
51. Y. Hwang, H. Li, B. A. E. Courtright, S. Subramaniyan and S. A. Jenekhe, *Adv. Mater.*, **28**, 124 (2016).
52. W. Zhao, D. Qian, S. Zhang, S. Li, O. Inganäs, F. Gao and J. Hou, *Adv. Mater.*, **28**, 4734 (2016).
53. B. Qui, L. Xue, Y. Yang, H. Bin, Y. Zhang, C. Zhang, M. Xiao, K. Park, W. Morrison, Z.-G. Zhang and Y. Li, *Chem. Mater.*, **29**, 7543 (2017).
54. L. Gao, Z.-G. Zhang, H. Bin, L. Xue, Y. Yang, C. Wang, F. Liu, T. P. Russell and Y. Li, *Adv. Mater.*, **28**, 8288 (2016).
55. N. Gasparini, M. Salvador, T. Heumuller, M. Richter, A. Classen, S. Shrestha, G. J. Matt, S. Holliday, S. Strohm, H.-J. Egelhaaf, A. Wadsworth, D. Baran, I. McCulloch and C. J. Brabec, *Adv. Energy Mater.*, **7**, 1701561 (2017).
56. E. Ko, G. Park, J. Lee, H. Kim, D. Lee, H. Ahn, M. A. Uddin, H. Woo, M. Cho and D. Choi, *ACS Appl. Mater. Interfaces*, **9**, 8838 (2017).
57. Y. Ma, M. Zhang, Y. Tang, W. Ma and Q. Zheng, *Chem. Mater.*, **29**, 9775 (2017).
58. G. Park, S. Choi, S. Park, D. Lee, M. Cho and D. Choi, *Adv. Energy Mater.*, **7**, 1700566 (2017).
59. P. Cheng, H. Bai, N. K. Zawacka, T. R. Anderson, W. Liu, E. Bundgaard, M. Jorgensen, H. Chen, F. C. Krebs and X. Zhan, *Adv. Sci.*, **2**, 1500096 (2015).
60. Q.-Y. Li, J. Xiao, L.-M. Tang, H.-C. Wang, Z. Chen, Z. Yang, H.-L. Yip and Y.-X. Xu, *Org. Electron.*, **44**, 217 (2017).
61. Y. Kim, D. Chung and C. Park, *Nano Energy*, **15**, 343 (2015).
62. S. Holiday, R. S. Ashraf, A. Wadsworth, D. Baran, S. A. Yousaf, C. B. Nielsen, C.-H. Tan, S. D. Dimitrov, N. Gasparini, M. Alamoudi, F. Laquai, C. J. Brabec, A. Salleo, J. R. Durrant and I. McCulloch, *Nat. Commun.*, **7**, 11585 (2016).
63. Z. Shi, H. Liu, Y. Wang, J. Li, Y. Bai, F. Wang, X. Bian, T. Hayat, A. Alsaedi and Z. Tan, *ACS Appl. Mater. Interfaces*, **9**, 43871 (2017).
64. S. Chambon, A. Rivaton, J.-L. Gardette and M. Firon, *Polym. Degrad. Stab.*, **96**, 1149 (2011).
65. A. Rivaton, S. Chambon, M. Manceau, J.-L. Gardette, N. Lemaître and S. Guillerez, *Polym. Degrad. Stab.*, **95**, 278 (2010).
66. M. Manceau, A. Rivaton, J.-L. Gardette, S. Guillerez and N. Lemaître, *Polym. Degrad. Stab.*, **94**, 898 (2009).
67. A. Tournebize, P.-O. Bussière, P. Wong-Wah-Chung, S. Thérias, A. Rivaton, J.-L. Gardette, S. Beaupré and M. Leclerc, *Adv. Energy Mater.*, **3**, 478 (2013).
68. I. Fraga Domínguez, P. D. Topham, P.-O. Bussière, D. Bégué and A. Rivaton, *J. Phys. Chem. C*, **119**, 2166 (2015).
69. A. Tournebize, P.-O. Bussière, A. Rivaton, J.-L. Gardette, H. Medlej, R. C. Hiorns, C. Dagron-Lartigau, F. C. Krebs and K. Norrman,

Chem. Mater., **25**, 4522 (2013).
70. R. Grisorio, G. Allegretta, P. Mastrorilli and G. P. Suranna, *Macromolecules*, **44**, 7977 (2011).
71. W. Zhao, S. Li, S. Zhang, X. Liu and J. Hou, *Adv. Mater.*, **29**, 1604059 (2016).
72. S. Li, L. Ye, W. Zhao, X. Liu, J. Zhu, H. Ade and J. Hou, *Adv. Mater.*, **29**, 1704051 (2017).
73. Q. Guan, R. Peng, Z. Liu, W. Song, R. Yang, L. Hong, T. Lei, Q. Wei and Z. Ge, *J. Mater. Chem. A*, **6**, 464 (2018).
74. X. Liu, L. Ye, W. Zhao, S. Zhang, S. Li, G. M. Su, C. Wang, H. Ade and J. Hou, *Mater. Chem. Front.*, **1**, 2057 (2017).